



A novel ratiometric two-photon fluorescent probe for imaging of Pd²⁺ ions in living cells and tissues



Liyi Zhou^{a,b,c,*}, Shunqin Hu^a, Haifei Wang^a, Hongyan Sun^c, Xiaobing Zhang^b

^a College of Packaging and Materials Engineering, Hunan University of Technology, Hunan 412007, PR China

^b Molecular Sciences and Biomedicine Laboratory, State Key Laboratory for Chemo/Biosensing and Chemometrics, College of Chemistry and Chemical Engineering, Collaborative Innovation Center for Chemistry and Molecular Medicine, Hunan University, Changsha 410082, PR China

^c Department of Biology and Chemistry, City University of Hong Kong, 83 Tat Chee Avenue, Kowloon, Hong Kong, PR China

ARTICLE INFO

Article history:

Received 7 March 2016

Received in revised form 5 May 2016

Accepted 11 May 2016

Available online 12 May 2016

Keywords:

Two-photon

Ratiometric fluorescent probe

Palladium

Fluorescent imaging

Naphthalimide derivative

ABSTRACT

Ratiometric two-photon fluorescent probes can not only eliminate interferences from environmental factors but also achieve deep-tissue imaging with improved spatial localization. To quantitatively track Pd²⁺ in biosystems, herein, we reported a ratiometric two-photon fluorescent probe, termed as Np-Pd, which based on a D-π-A-structure two-photon fluorophore of the naphthalimide derivative and deprotection of aryl propargyl ethers by palladium species. The probe Np-Pd displayed a more than 25-fold enhancement towards palladium species with high sensitivity and selectivity. Additionally, the probe Np-Pd was further used for fluorescence imaging of Pd²⁺ ions in living cells and tissues under two-photon excitation (820 nm), which showed large tissue-imaging depth (19.6–184.6 μm), and a high resolution for ratiometric imaging.

© 2016 Elsevier B.V. All rights reserved.

1. Introduction

Palladium, one of the platinum-group elements, has adverse effects on our health when it is taken into human bodies via contaminated food, medicine, and water [1–2]. Therefore, detection and removal of it have received intense attention for their significance in chemistry, biology, and environmental science [3]. In particular, palladium, can have adverse effects on our health and the environment, because DNA, proteins, and other biomacromolecules, such as vitamin B6, have been reported to be able to strongly bind it, which may lead to a variety of cellular dysfunction processes [4]; additionally, palladium is as well as often used to prepare dental materials, electric equipment, jewelry, and automobile exhaust catalysts [5]. Wherefore, this led to the urgent need to develop an efficient method of detecting Pd²⁺ ions both in the living and environmental setting.

So far, several analytical techniques have been developed for the efficient analysis and detection of palladium species, such as inductively coupled plasma mass spectrometry (ICP-MS), atomic absorption spectrometry (AAS), inductively coupled plasma emission spectroscopy (ICP-AES), X-ray fluorescence (XRF), and so on [6]. Although these methods are sensitive towards palladium, they usually require

expensive instruments and high skilled professionals. In contrast, fluorescent probes can maintain comparable efficiency and accuracy to avoid these shortcomings. Therefore, they have been widely exploited by researchers for the detection of a variety of bio-related substances. To date, only a few fluorescent probes have been reported for quantitative detection of Pd²⁺ concentration [7]. Unfortunately, most of these fluorescent probes are excited by one-photon excitation with a short wavelength, which results in some obvious drawbacks for bioimaging, such as high autofluorescence background, photobleaching, and shallow tissue-penetration depth. Moreover, most of these probes are based on a single emission peak, which tends to be affected by a variety of factors, including instrumental variations, environmental condition changes, and probe concentration changes. Therefore, developing a simple and reliable fluorescent probe for the quantitative detection of the Pd²⁺ concentration not only in living cells but also in living tissues is of great significance and necessity.

To solve these problems, we used an effective two-photon fluorescence microscopy (TPFM) approach, in which a two-photon (TP) fluorescent dye was excited by a long-wavelength laser light and thus provided a variety of advantages compared with traditional confocal microscopy [8]. It can improve the three-dimensional imaging of living tissues, reduce photodamage to biosamples, increase tissue penetration, and lower background fluorescence. Additionally, associating with a ratiometric strategy, the built-in correction of the two emission bands could further eliminate interference caused by instrumental variations, environmental factors, and probe concentrations [9].

* Corresponding author at: College of Packaging and Materials Engineering, Hunan University of Technology, Hunan 412007, PR China.
E-mail address: zhouly0817@163.com (L. Zhou).

Recently, 4-hydroxy-naphthalimide derivative have been reported as an efficient two-photon platform for designing two-photon probes with its tunable two-photon properties because of the hydroxyl group [10]. Herein, we used this platform further to develop a new ratiometric two-photon fluorescent probe, Np-Pd, for Pd²⁺ ion detection and bioimaging applications. The probe Np-Pd showed two well-separated fluorescence emission peaks (445 nm and 550 nm), which provided a large signal-to-background ratio of 26, and therefore high sensitivity of the probe with a detection limit of 2.8×10^{-7} mol/L observed for Pd²⁺ ions. It exhibited a pronounced ratiometric signal changes as the deprotection of aryl propargyl ethers in the presence of Pd²⁺ ions, and large tissue-imaging depths with a high resolution for ratiometric imaging by TPFM.

2. Experimental

2.1. Reagents and apparatus

Unless otherwise specified, all chemicals were obtained from commercial suppliers and used without further purification. Thin layer chromatography (TLC) was carried out using silica gel 60 F254, and column chromatography was conducted over silica gel (100–200mesh), both of them were obtained from Qingdao Ocean Chemicals (Qingdao, China). In all experiments, water used was doubly distilled and purified by a Milli-Q system (Millipore, USA). LC-MS analyses were performed using an Agilent 1100 HPLC/MSD spectrometer. Mass spectra were performed using an LCQ Advantage ion trap mass spectrometer (Thermo Finnigan). ¹HNMR spectra were obtained using a Bruker DRX-400 spectrometer using TMS as an internal standard. All chemical shifts are reported in the standard δ notation of parts per million. UV-vis absorption spectra were recorded in 1.0 cm path length quartz cuvettes on a Shimadzu 2450 UV-visible Spectrometer. Fluorescence measurements were carried out on a F4500 fluorescence spectrometer with excitation and emission slits set at 5.0 nm and 5.0 nm, respectively. The pH was measured with a Mettler-Toledo Delta 320 pH meter.

2.2. Synthesis of probe molecule Np-O, and Np-Pd

Synthesis of Np-Br: 2.57 g (0.01 mol) **compound 1** and 1.8 g (0.011 mol) 4-bromo aniline was dissolved in 100 mL of CH₃COOH, the mixture was refluxed for 4 h, then poured into ice-water, the solid was washed with HCl_(aq.) and NaOH_(aq.), respectively, and then the gray white solid was obtained via the vacuum pump leak and dried under the vacuum oven. ¹HNMR(400 MHz, *d*₆-DMSO) δ (ppm) = 10.07 (s, 1H), 8.63–8.59 (t, *J* = 4 Hz, 1H), 8.35–8.26 (t, *J* = 18 Hz, 1H), 8.03 (s, 1H), 7.76–7.74 (d, *J* = 4 Hz, 1H), 7.56–7.54 (d, *J* = 4 Hz, 1H), 7.48–7.39 (m, 4H), +C ESI ms = 432.3, calcd = 431.0.

According to the literature to synthesize 4-hydroxyl group naphthalene imide (Np-O) [11]: **Np-O:** ¹HNMR (400 MHz, *d*₆-DMSO) δ (ppm) = 11.97 (s, 1H), 8.59–8.53 (3H), 8.71–7.17 (6H), +C ESI ms = 368.4, calcd = 368.2.

Synthesis of Np-Pd: 184 mg (0.5 mmol) **Np-O**, 138 mg (1 mmol) K₂CO₃, 118 mg (1 mmol) 3-bromoprop-1-yne, and 50 mL CH₃CN were added into a round bottom flask, the mixture was reacted for 4 h at 50 °C, then poured into ice-water, the solid was washed with water three times, and then the white solid was obtained in 95% yield via the vacuum pump leak and dried under the vacuum oven. ¹HNMR (400 MHz, *d*₆-DMSO) δ (ppm) = 8.59–8.47 (m, 3H), 7.89–7.85 (t, *J* = 8 Hz, 1H), 7.71–7.67 (d, *J* = 16 Hz, 2H), 7.44–7.35 (m, 4H), 5.24 (s, 1H), 3.33 (s, 1H), +C ESI ms = 408.3, calcd = 406.2.

2.3. Two-photon excited fluorescence measurement

The two-photon excited fluorescence was measured by using a Ti:sapphire femtosecond oscillator (SpectraPhysics Mai Tai) as the excitation source. The output laser pulses have a tunable central wavelength

from 690 nm to 1020 nm with pulse duration of less than 100 fs and a repetition rate of 80.5 MHz. The laser beam was focused onto the samples using a lens with a focus length of 3.0 cm. The emission was collected at an angle of 90° to the direction of the excitation beam to minimize the scattering. The emission signal was directed into a CCD (Princeton Instruments, Pixis 400B) coupled monochromator (IsoPlane160) with an optical fiber. A 750 nm short pass filter was placed before the spectrometer to minimize the scattering from the excitation light. The two photon absorption (TPA) cross section (δ) of the sample (s) at each wavelength was calculated according to Equation (1), and rhodamine B in CH₃OH was used as the reference (r) [12].

$$\delta = \delta_r (S_s \Phi_r f_r c_r) / (S_r \Phi_s f_s c_s) \quad (1)$$

where *S* is the integrated fluorescence intensity, Φ is the fluorescence quantum yield, *C* is the concentration of sample (s) and reference (r), and ϕ is the collection efficiency of the experimental setup. The uncertainty in the measurement of cross sections is ~15%. The detailed calculation is given in the Supplementary data (Fig. S1).

2.4. Spectrophotometric measurements

The fluorescence measurement experiments were measured in phosphate buffer solution (10 mM) with DMSO as co-solvent solution (H₂O/ DMSO = 99:1, v/v). The pH value of PBS solution used was from 3.0 to 10, which was achieved by adding minimal volumes of HCl solution or NaOH solution. The fluorescent emission spectra were recorded at excitation wavelength of 375 nm with emission wavelength range from 425 to 650 nm. A 1×10^{-3} mol/L stock solution of probe was prepared by dissolving probe compound in DMSO. Procedure of calibration measurements with probe in the buffer with different pH followed: 20 μ L stock solution of probe and 1980 μ L PBS buffer solution with different pH were combined to afford a test solution, which contained 1×10^{-6} mol/L of probe. The solutions of various testing species were prepared from NaCl, CaCl₂, MgSO₂, CuCl₂·H₂O, Zn(NO₃)₂·6H₂O, using twice-distilled water with final concentrations of 0.0125 mol/L, as well as, glutathione (GSH), cysteine (Cys), and glutamate (Glu) using twice-distilled water with final concentrations of 0.025 M. Procedure of selectivity experiments followed: for cations or anions, 20 μ L stock solution of probe, 1948 μ L PBS solution (pH 7.4) and 32 μ L solution of each cation or anion were combined to afford a test solution, which contained 1×10^{-6} mol/L of probe and 100 μ M cation or anion; for amino acids, 20 μ L stock solution of probe, 1900 μ L PBS buffer solution (pH 7.4) and 80 μ L solution of each amino acid were combined to afford a test solution, which contained 1×10^{-6} mol/L of probe and 100 μ M amino acid.

2.5. HPLC analysis

1 μ M of Np-Pd in DMF (2.0 mL) and 1 μ M of Np-O in buffered (10 mM PBS, pH 7.4) DMF/ H₂O solution (1:99, v/v) were prepared as the control solution. The reaction solution (2.0 mL) was prepared with 5 μ M Np-Pd in buffered DMF/H₂O solution incubated for 30 min at 37 °C after addition of Pd²⁺ ions (50 eq.). An aliquot of each solution (100 μ L) was loaded onto an Inertsil ODS-3 (250 mm \times Φ 4.6 mm) C18 column (GL Sciences, Inc.) fitted on an Agilent 1260 Infinity HPLC system, and the eluates were monitored with a photodiode array detector. Detection wavelength was kept at 330 nm, and flow rate was set at 1.0 mL/min. Milli-Q water containing 0.1% TFA (A) and MeCN (B) were used as developing solvents. Gradient conditions were chosen as follows: 10% A and 90% B for 15 min.

2.6. Cell cytotoxic assays and imaging

The cytotoxic effects of the probe were assessed using MTT assays. Fluorescent images of cells and tissues were obtained using Olympus

FV1000-MPE multiphoton laser scanning confocal microscope (Japan). For fluorescent imaging, the cells were washed with PBS buffer followed by incubation with the probe (5 μM) for 30 min in culture medium (PBS buffer containing 1% DMSO) at 37 $^{\circ}\text{C}$. Cell samples were then washed with PBS three times and imaged. Pd^{2+} ions (20 μM) were added to induce a ratiometric signal change during imaging. The two-photon excitation wavelength of the femtosecond laser was fixed at 820 nm; the emission wavelengths were recorded at (420–460) nm, (520–570) nm, respectively.

2.7. Preparation and staining of mouse liver tissue slice

The mouse liver tissue slice were cultured with 10 μM Np-Pd in an incubator at 37 $^{\circ}\text{C}$ for 1 h and washed with PBS three times, following, the slices were added 50 μM Pd^{2+} for another 1 h and then washed with PBS three times for TPFM imaging. The TPFM images (with a magnification at 10 \times) were collected in two channels (blue = 420–460 nm, yellow = 520–570 nm) upon excitation at 820 nm with a pulse laser.

3. Results and discussion

3.1. Design and synthesis of probe molecule Np-Pd

We employ a previously reported D- π -A-structured 4-hydroxy-naphthalimide platform to design an efficient ratiometric two-photon fluorescence probe for Pd^{2+} ions. In our designed probe Np-Pd, exhibiting a pronounced ratiometric signal changes as the deprotection of aryl propargyl ethers in the presence of Pd^{2+} ions (Scheme 1). On the basis of previously reported, Np-Pd was prepared in 95% yield by the coupling of Np-O with 3-bromo-1-propyne in a one-pot method. The detailed synthetic procedure is described in Scheme 1, and all the chemical structures of compounds were verified by Mass, ^1H NMR spectroscopy, seen in the Supporting information.

3.2. Optical property and selectivity of Np-Pd

The spectroscopic properties of Np-Pd (5 μM) were examined in phosphate buffer solution (10 mM, pH 7.4, 99:1 H_2O /DMSO, v/v) with different Pd^{2+} ion concentrations. The probe displays sensitive absorption (Fig. 1A) and fluorescence (Fig. 1B) responses to changes in Pd^{2+} ion concentration. As shown in Fig. 1A, in the absence of Pd^{2+} ions, only one absorption peak was observed at the maximum absorption wavelength ($\lambda = 350$ nm). After Pd^{2+} ions (0–50 μM) were added, a new absorption peak appeared at 470 nm. Further fluorescence experiments showed a dramatic increase in fluorescence intensity at $\lambda_{\text{em}} = 550$ nm and an obvious decrease in fluorescence intensity at $\lambda_{\text{em}} = 445$ nm (Fig. 1B). $F_{550/445}$ was gradually increased from 0.16 to 4.2 with the increasing concentration of Pd^{2+} changed from 0 to 50 μM , respectively, corresponding to a signal-to-background ratio of 26, which provided the basis for high-performance ratiometric (F_{550}/F_{445}) detection and exhibited an excellent F_{550}/F_{445} linearity towards different

Pd^{2+} concentration (0–1.0 μM) (Fig. 1D). What's more, in the present study, the detection limit (3 σ /slope) [7h] was estimated to be as low as 2.8×10^{-7} mol/L for Pd^{2+} , which is sufficiently low for the detection of the submillimolar concentration range of Pd^{2+} found in many chemical and biological systems. The fluorescence enhancement response of Np-Pd to Pd^{2+} is most likely the result of the conversion of probe Np-Pd to compound Np-O (Scheme 1). To verify the proposed mechanism, the change of UV–vis absorption spectra and HPLC spectra of Np-Pd upon the addition of Pd^{2+} were first investigated (Fig. 1A and Fig. S2). To further verify this hypothesis, the purified product of the reaction of Np-Pd with Pd^{2+} ions was then characterized by NMR, which agreed well with the presynthesized Np-O, directly indicating the correct of our proposed mechanism.

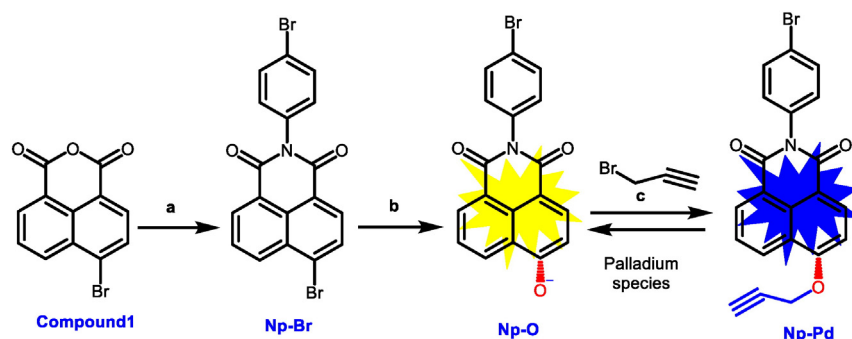
3.3. Selectivity, Effect of pH and time-dependent fluorescence response

High selectivity and suitable pH working range are an important parameter to evaluate a newly designed fluorescent probe performance. Np-Pd was treated with a wide variety of analytes to examine its selectivity. As shown in Fig. 2A (black bars), the addition of Pd^{2+} induced a significant red-shift of the fluorescence emission spectra. However, upon treatment with 10 equivalents of other analytes the fluorescence intensities almost had no changes, even if after a very long reaction time. So, via the selectivity experiments, we found that only Pd^{2+} ions could respond to the probe Np-Pd, whereas other ions showed no perceptible effect, demonstrating high selectivity of the probe towards Pd^{2+} ions. Competition experiments were also carried out to assess the practical applicability of the probe. Ten equivalent of other metal ions or neutral molecules is added to 50 μM of Pd^{2+} separately, and the fluorescence response of the probe is then recorded with the results shown in Fig. 2A (red bars). The probe showed almost unchanged fluorescent responses to Pd^{2+} before and after the addition of other interfering metal ions or neutral molecules. These results demonstrated that our Np-Pd probe could meet the selective requirements for practical applications.

We also studied the effect of pH on Np-Pd in the absence and presence of Pd^{2+} ions (Fig. 2B). Without Pd^{2+} ions, no obvious characteristic fluorescence of the acceptor could be observed from pH 3.0 to 10.0. Upon addition of Pd^{2+} ions, the best response towards Pd^{2+} could be achieved with a pH range from 4.0 to 10.0. Thus, the PBS solution (pH 7.4) was used throughout the experiment. These results indicated that the probe was favorable for applications in practical samples at different pH values. What's more, Np-Pd possesses a quick fluorescent response time within 5 min, which could ensure detection of low concentration of Pd^{2+} in living systems with a fast response time (Fig. 2C).

3.4. Two-photon active absorption cross-section measurement

Naphthalimide derivative exhibit excellent two-photon properties with a two-photon action cross-section, showing this two-photon dye



Scheme 1. Structure of Np-Pd and its response mechanism to palladium species.

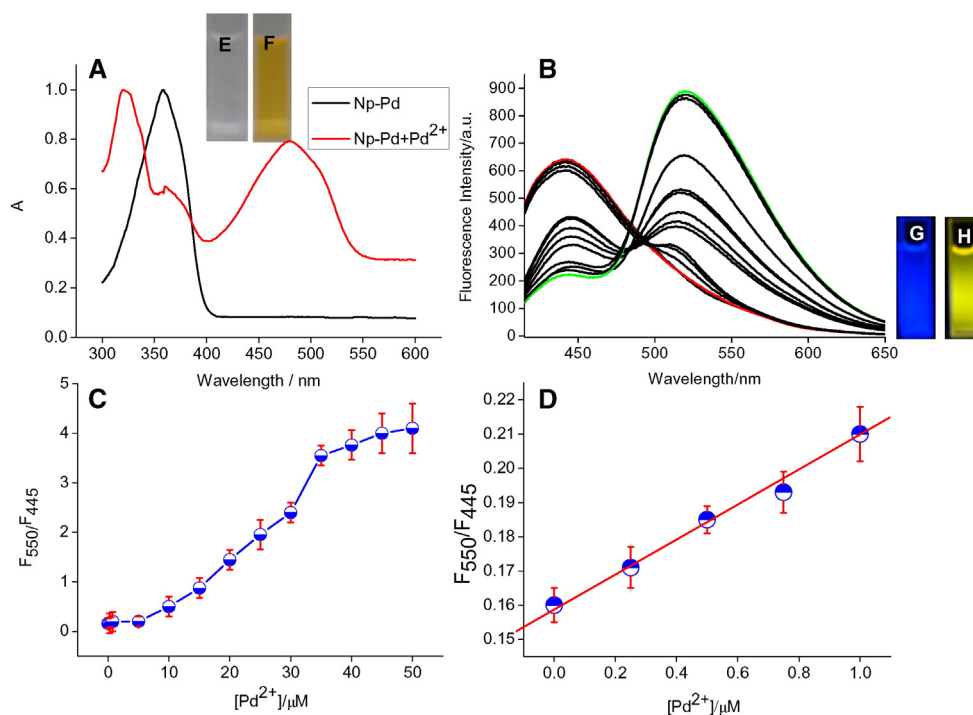


Fig. 1. (A) Absorption spectra of 5 μM Np-Pd and 5 μM Np-Pd + 50 μM Pd^{2+} ions; (B) Fluorescence spectra of 5 μM Np-Pd in the presence of increasing concentrations of Pd^{2+} ions (0–50 μM); (C) Calibration curve of Np-Pd to Pd^{2+} ions. The curve was plotted with the fluorescence intensity vs Pd^{2+} ion concentration (0–50 μM); (D) Linear relationship between F_{550}/F_{445} and Pd^{2+} ion concentration in the 0–1.0 μM range; (E and F) Change in color of the probe before and after the addition of 50 μM Pd^{2+} ions in 5 μM of Np-Pd in 99:1 PBS/DMSO, pH 7.4; (G and H) Change in the fluorescence of the probe before and after the addition of 50 μM Pd^{2+} ions in 5 μM of Np-Pd under excitation by UV light.

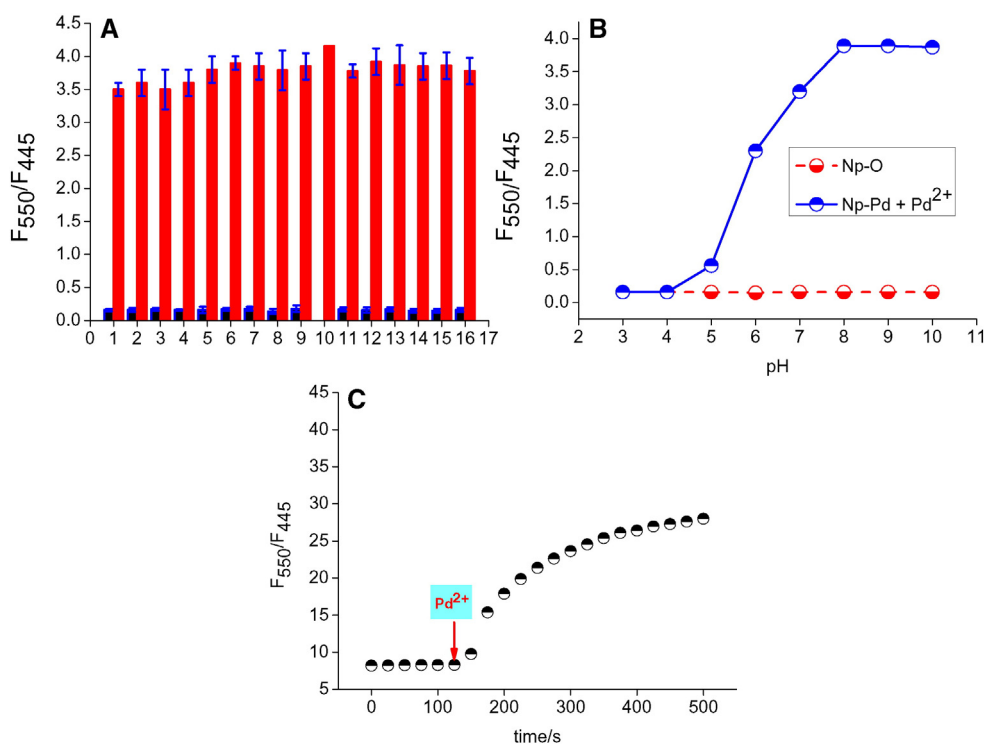


Fig. 2. (A) Fluorescence response of 5 μM Np-Pd to 50 μM of Pd^{2+} or 10 equivalents of other metal ions or neutral molecules (pink bars) and to the mixture of 10 equivalents of other divalent metal ions or neutral molecules with 50 μM of Pd^{2+} (brick red bars); (B) pH effects on Np-Pd in the absence or presence of Pd^{2+} . The numbers from 1 to 16 correspond to GSH to Fe^{3+} , respectively (GSH, Cys, Glu, Pb^{2+} , Hg^{2+} , Ca^{2+} , Mg^{2+} , Co^{2+} , Cu^{2+} , Pd^{2+} , Ni^{2+} , Cr^{3+} , Zn^{2+} , Al^{3+} , Na^{+} , and Fe^{3+}); (C) Time-dependent fluorescence response records of 5 μM Np-Pd in 10 mM PBS solution (1% DMSO, pH 7.4) upon additions of 50 μM Pd^{2+} ions solution. (For interpretation of the references to color in this figure legend, the reader is referred to the web version of this article.)

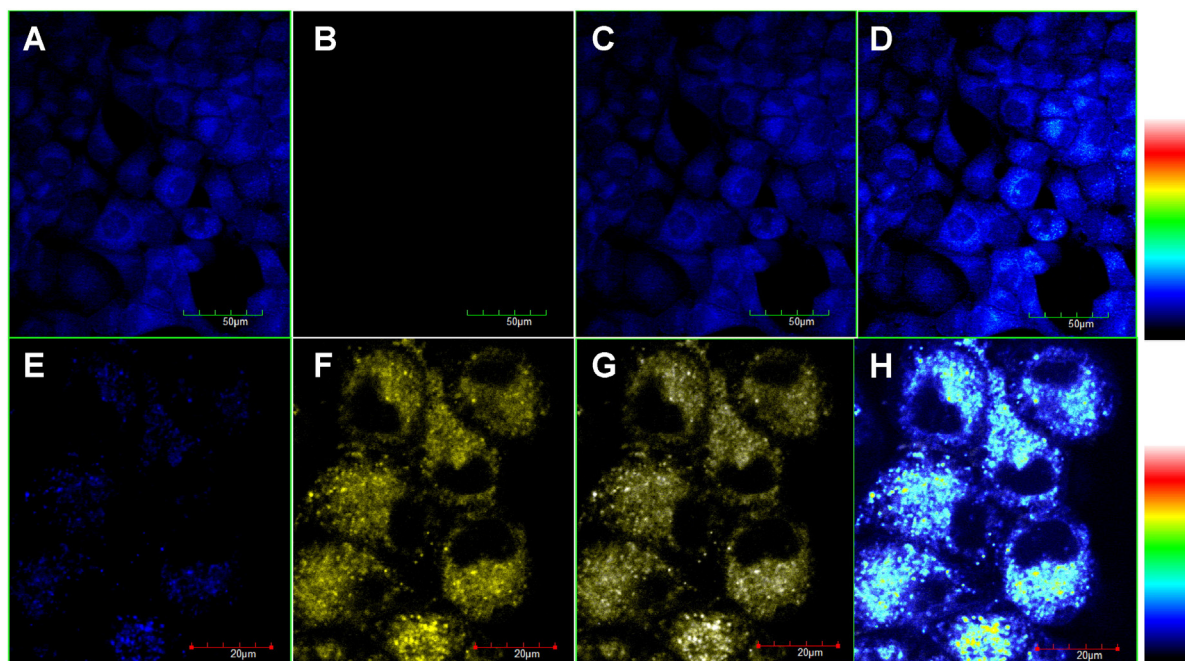


Fig. 3. TP-excited ratiometric fluorescence images of 5 μM Np-Pd in 10 mM PBS in HeLa cells stimulated with or without Pd^{2+} ions. TP images from the blue channel (A) and the yellow channel (B) without Pd^{2+} ions; (C) Merged images of (A) and (B); (D) Ratiometric images of (A) and (B); (E) Two-photon images from the blue channel and (F) the yellow channel with Pd^{2+} ions; (G) Merged images of (E) and (F); (H) Ratiometric images of (E) and (F). Two-photon images: $\lambda_{\text{ex}} = 820$ nm. Blue channel: $\lambda_{\text{em}} = 420\text{--}460$ nm; yellow channel: 520–570 nm. Scale bar: (A–D) 50 μm , and (E–H) 20 μm . (For interpretation of the references to color in this figure legend, the reader is referred to the web version of this article.)

is potentially useful for bioimaging applications. For our probe Np-Pd, in the absence of Pd^{2+} ions, the Np-Pd was calculated to have a two-photon active absorption cross-section of 78GM ($1\text{GM} = 10^{-50}(\text{cm}^4 \text{s})/\text{photon}$) at 445 nm upon excitation at 820 nm (Fig. S1, the red line). In

the presence of Pd^{2+} ions, the Np-O was calculated to have a two-photon active absorption cross-section of 70GM, as well as a new strong fluorescent peak appeared at 550 nm (Fig. S1, the black line).

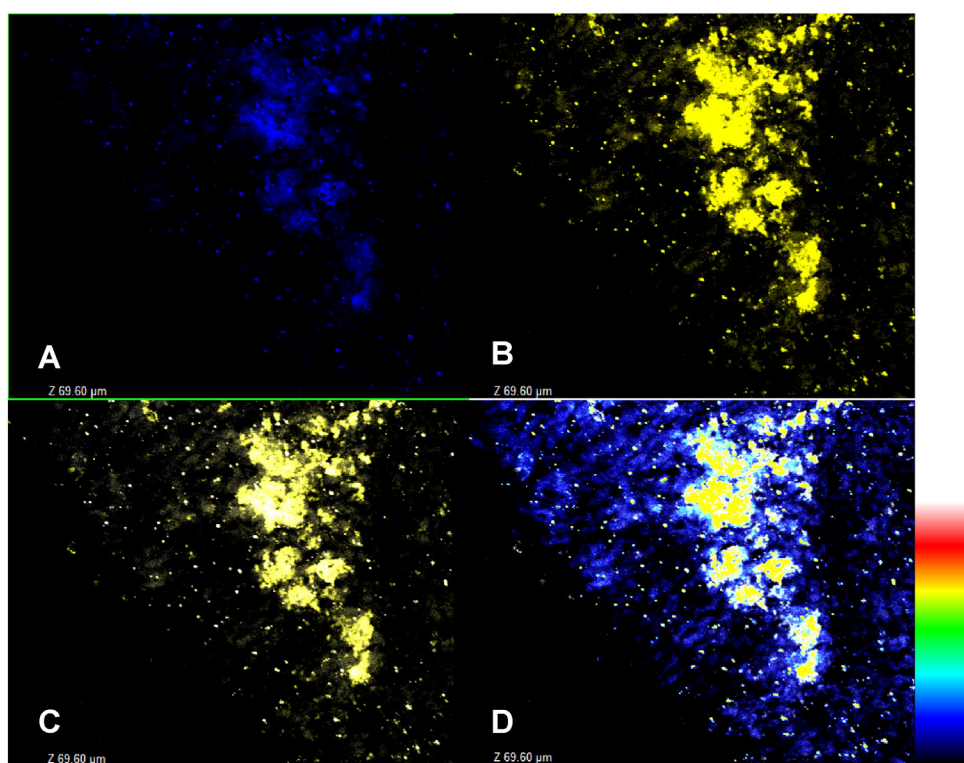


Fig. 4. TPFM images of a frozen liver tissue slice from a nude mouse stained with 10 μM Np-Pd at 69.6 μm for 60 min followed by treatment with 50 μM Pd^{2+} and incubated for another 60 min (A, B); (C) Overlay image of (A) and (B); (D) Ratiometric image of (A) and (B). The images were collected at 420–460 nm (blue channel, A) and 520–570 nm (yellow channel, B) upon excitation at 820 nm with femtosecond pulses. Scale bar: 50 μm . (For interpretation of the references to color in this figure legend, the reader is referred to the web version of this article.)

3.5. Ratiometric two-photon imaging in living cells

To demonstrate the practical applicability of the probe in biological systems, we carried out fluorescence imaging experiments in living cells (HeLa cells). The cytotoxicity of the probe was first evaluated by using MTT assays for HeLa cells. Experimental results demonstrated that the Np-Pd probe exhibited negligible cytotoxicity to the cell lines (Fig. S3 in the Supporting information). Before two-photon fluorescent imaging, cells were incubated with 5 μM Np-Pd at 37 $^{\circ}\text{C}$ for 30 min, which then exhibited strong two-photon intracellular fluorescence in blue channel (Fig. 3A) and weak fluorescence in the yellow channel (Fig. 3B). These results demonstrated that Np-Pd could penetrate the cell membrane. However, incubation of the cells with 20 μM of Pd^{2+} ions could significantly decrease the two-photon excited fluorescence signal in the blue channel (Fig. 3E) but with an enhancement of the two-photon excited fluorescence signal in the yellow channel (Fig. 3F). These preliminary experimental results demonstrated that Np-Pd could be successfully applied for two-photon-excited ratiometric imaging of Pd^{2+} ions in live cells.

3.6. Tissues slice ratiometric imaging

Np-Pd was further applied for TP-excited fluorescence imaging of Pd^{2+} ions in liver tissue slices from nude mice with images at different tissue depths recorded by TPFM in the Z-scan mode. Experimental results indicated that the probe could be successfully applied for ratiometric imaging of Pd^{2+} ions in tissue at a depth of 19.6–184.6 μm in dual-channels at two well-separated wavelengths (see Fig. 4 and Fig. S4 in the Supporting information). These results demonstrated that the probe possessed a good staining capability and high penetrating ability in tissue as well as high resolution for two-color ratiometric imaging.

4. Conclusion

In summary, we have designed and synthesized a novel robust ratiometric two-photon fluorescent probe, termed Np-Pd, for detecting Pd^{2+} ions not only in living cells but also in living tissues. Np-Pd is based on a two-photon fluorophore 4-hydroxyl group naphthalimide. In probe Np-Pd, it shows a ratiometric signal changes as the deprotection of aryl propargyl ethers in the presence of Pd^{2+} ions. The experiments demonstrate that Np-Pd possesses high ratiometric imaging resolution and large tissue-imaging depth (19.6–184.6 μm) at the cellular and tissue levels. We believe that Np-Pd could find wide applications not only in environmental monitoring but also biomedical diagnostics for Pd^{2+} ions.

Acknowledgements

This work was supported by Natural Science Foundation of China (NSFC, Grants 21202042), Hunan Provincial Natural Science Foundation of China (Grant 13JJ4090).

Appendix A. Supplementary data

Supplementary data to this article can be found online at <http://dx.doi.org/10.1016/j.saa.2016.05.013>.

References

- [1] (a) J.C. Wataha, C.T. Hanks, *J. Oral Rehabil.* 23 (1996) 309–320; (b) J. Kielhorn, C. Melber, D. Keller, I. Mangelsdorf, *Health* 205 (2002) 417–432.
- [2] B. Liu, H. Wang, T. Wang, Y. Bao, F. Du, J. Tian, Q. Li, R. Bai, *Chem. Commun.* 48 (2012) 2867–2869.
- [3] T. Schwarze, H. Müller, C. Dosche, T. Klamroth, W. Mickler, A. Kelling, H.G. Löhmansröben, P. Saalfrank, H.J. Holdt, *Angew. Chem. Int. Ed.* 46 (2007) 1671–1674.
- [4] (a) T. Gebel, H. Lantzsch, K. Plebow, H. Dunkelberg, *Mutat. Res. Genet. Toxicol. Environ. Mutagen.* 389 (1997) 183–190; (b) C.L. Wise-man, F. Zereini, *Sci. Total Environ.* 407 (2009) 2493–2500; (c) C.D. Spicer, T. Triemer, B.G. Davis, *J. Am. Chem. Soc.* 134 (2012) 800–803; (d) R.M. Yusop, A. Unciti-Broceta, E.M.V. Johansson, R.M. Sánchez-Martín, M. Bradley, *Nat. Chem.* 3 (2011) 239–243.
- [5] M. Paraskevas, F. Tsopelas, M. Ochsenkühn-Petropoulou, *Microchim. Acta.* 176 (2012) 235–242.
- [6] (a) O.V. Borisov, D.M. Coleman, K.A. Oudsema, R.O. Carter III, *J. Anal. At. Spectrom.* 12 (1997) 239–246; (b) B. Dimitrova, K. Benkhedda, E. Ivanova, F. Adams, *J. Anal. At. Spectrom.* 19 (2004) 1394–1396; (c) C. Locatelli, D. Melucci, G. Torsi, *Anal. Bioanal. Chem.* 382 (2005) 1567–1573; (d) K. Van Meel, A. Smekens, M. Behets, P. Kazandjian, R. VanGrieken, *Anal. Chem.* 79 (2007) 6383–6389.
- [7] (a) S. Sun, B. Qiao, N. Jiang, J. Wang, S. Zhang, X. Peng, *Org. Lett.* 16 (2014) 1132–1135; (b) F. Song, A.L. Garner, K. Koide, *J. Am. Chem. Soc.* 129 (2007) 12354–12355; (c) A.L. Garner, F. Song, K. Koide, *J. Am. Chem. Soc.* 131 (2009) 5163–5171; (d) W. Guo, L. Wang, J. Jiao, J. Hou, Y. Cheng, C. Zhu, *Tetrahedron Lett.* 53 (2012) 3459–3462; (e) M. Yang, Y. Bai, W. Meng, Z. Cheng, N. Su, B. Yang, *Inorg. Chem. Commun.* 46 (2014) 310–314; (f) J. Zhang, L. Zhang, Y. Zhou, T. Ma, J. Niu, *Microchim. Acta* 180 (2013) 211–217; (g) Y. Zhou, J. Zhang, H. Zhou, Q. Zhang, T. Ma, J. Niu, *Sensors Actuators B Chem.* 171–172 (2012) 508–514; (h) B.C. Zhu, C.C. Gao, Y.Z. Zhao, C.Y. Liu, Y.M. Li, Q. Wei, Z.M. Ma, B. Du, X.L. Zhang, *Chem. Commun.* 47 (2011) 8656–8658; (i) H. Li, J. Fan, X. Peng, *Chem. Soc. Rev.* 42 (2013) 7943–7962; (j) H. Cui, H. Chen, Y. Pan, W. Lin, *Sensors Actuators B* 219 (2015) 232–237; (k) W. Liu, J. Jiang, C. Chen, X. Tang, J. Shi, P. Zhang, K. Zhang, Z. Li, W. Dou, L. Yang, W. Liu, *Inorg. Chem.* 53 (2014) 12590–12594.
- [8] (a) H.M. Kim, B.R. Cho, *Chem. Asian. J.* 6 (2011) 58; (b) H.M. Kim, B.R. Cho, *Acc. Chem. Res.* 42 (2009) 863–872.
- [9] (a) Z.C. Xu, K.H. Baek, H.N. Kim, J.N. Cui, X.H. Qian, D.R. Spring, I.J. Shin, J.Y. Yoon, *J. Am. Chem. Soc.* 132 (2010) 601–610; (b) Z.X. Han, X.B. Zhang, Z. Li, Y.J. Gong, X.Y. Wu, Z. Jin, C.M. He, L.X. Jian, J. Zhang, G.L. Shen, R.Q. Yu, *Anal. Chem.* 82 (2010) 3108–3113; (c) Y. Zhao, X.B. Zhang, Z.X. Han, L. Qiao, C.Y. Li, L.X. Jian, G.L. Shen, R.Q. Yu, *Anal. Chem.* 81 (2009) 7022–7030; (d) C.Y. Li, X.B. Zhang, L. Qiao, Y. Zhao, C.M. He, S.Y. Huan, L.M. Lu, L.X. Jian, G.L. Shen, R.Q. Yu, *Anal. Chem.* 81 (2009) 9993–10001.
- [10] (a) T. Liu, X. Zhang, Q. Qiao, C. Zou, L. Feng, J. Cui, Z. Xu, *Dyes Pigments* 99 (2013) 537–542; (b) Z.R. Dai, G.B. Ge, L. Feng, J. Ning, L.H. Hu, Q. Jin, D.D. Wang, X. Lv, T.Y. Dou, J.N. Cui, L. Yang, *J. Am. Chem. Soc.* 137 (2015) 14488–14495.
- [11] W. Shu, L. Yan, J. Liu, Z. Wang, S. Zhang, C. Tang, C. Liu, B.D. Zhu, *Ind. Eng. Chem. Res.* 54 (2015) 8056–8062.
- [12] (a) C. Xu, W.W. Webb, *JOSA. B* 13 (1996) 481–491; (b) M.A. Albota, C. Xu, W.W. Webb, *Appl. Opt.* 37 (1998) 7352–7356.